# Cerebrospinal Fluid Flow Simulations during Head Nodding Motions

William W. Liou<sup>1,a)</sup>, Jin Xu<sup>1,b)</sup>, Yang Yang<sup>1,c)</sup> and Shinya Yamada<sup>2,d)</sup>

<sup>1</sup>Department of Mechanical and Aerospace Engineering, Western Michigan University, U.S.A. <sup>2</sup>Department of Neurosurgery, Juntendo University, Japan

a) Corresponding Author: William.liou@wmich.edu
b) Jin.xu@wmich.edu
c) Yang.yang@wmich.edu
d) Shinyakoro@gmail.com

**Abstract.** Computational simulations of the biofluid flow in the ventricles in the brain are performed using computational fluid dynamics method. The head movements considered are head nodding motions. The cerebrospinal fluid flow is modeled as a Newtonian fluid with properties at the core body temperature. The motions of the brain are associated with two head motions. One is the normal nodding that is customarily signaling agreement and the second represents a hypnogogic jerk. The results of the simulations show that the cerebrospinal fluid flows in the brain ventricle are moderately affected by the light nodding, but the effects are more significant during the hypnagogic jerk motion, where mixing of the cerebrospinal fluid is distinctly enhanced. The outcomes illustrate that the head motions are significant drivers of ventricular cerebrospinal fluid flow simulated.

Keywords. Cerebrospinal Fluid Flow, Nodding Motions, glymphatic system

### INTRODUCTION

Cerebrospinal fluid (CSF) is a neurofluid in the brain. With the specific gravity of about 1.007, CSF surrounds the brain in the subarachnoid space (SAS) in the cranial vault and protects the brain tissue from injury when jolted. CSF in SAS also allows the brain to be in a neutral buoyancy state and the brain to maintain its density without being impaired by its own weight. CSF flows in the four ventricles that are located deep inside the brain. The ventricles, including the paired lateral ventricles, the third ventricle, and the fourth ventricle, are interconnected, allowing the CSF to move freely in the ventricles and to the SAS. Flowing deep inside the brain, the flow of CSF in the ventricles performs many irreplaceable tasks that are critical to the functioning of the brain [1]. For instance, the ventricular CSF flow transports nutrients, hormones, and brain metabolites from where they are produced to target nucleuses, such as the circumventricular organs or to be removed from the brain through the glymphatic system.

For a brain at rest, CSF flow dynamics is a result of the interaction between the brain tissues, the vascular systems, and other factors, such as the cardiac cycle and respiration. The cranium's constituents maintain a homeostasis, such that any increase in the volume of one of the cranial constituents must be compensated by a decrease in the volume of the others. The pressure-volume relationship between the intracranial pressure (ICP), the volume of CSF, blood, and brain tissue, is known as the Monro-Kellie doctrine. In the systolic portion of the cardiac cycle, blood flows into the cranial vault, a nearly equal amount of the venous blood and CSF is pushed out of the vault, contributing to the pulsatile nature of the CSF flow dynamics, and the ICP is maintained. A current school of thought hypothesizes that there is a bulk CSF flow in the ventricular system [2]. According to such a hypothesis, the CSF forms largely in the lateral ventricles and flows through the foramen of Monro to the third ventricle, then caudally through the cerebral aqueduct, or aqueduct of Sylvius, to the fourth ventricle. The CSF then flows to the SAS through either the paired

lateral foramina of Luschka or the midline foramen of Magendie, and to the central canal of the spinal cord. The CSF exchange and mixing in the ventricles are observed in normal brain [3].

Computational models are being applied at increasing rate toward a better understanding and assessment of the circulation of biofluids, and prediction of deleterious human physiological effects. For instance, lumped-parameter based models were developed to provide representations of cardiovascular pathologies.1 Modeled hemodynamics using a lumped-parameter formulation provides beat-by-beat and long-duration information of the cardiac system and the renal system [1, 4]. This information has been extracted and used in various forms by researchers as the flow boundary conditions in unsteady, three-dimensional computational fluid dynamics (CFD) calculations of the modeled compartments [3, 5]. Through the use of mathematical models, CFD simulation makes available flow quantities, such as fluid flow velocity and pressure, that can be difficult, if not impossible, to measure in vivo in, for example, the CSF flow in the spinal or cranial compartments [6]. CFD simulations, using commercial software, of the CSF flow have also been reported by directly imposing measured flow volume and velocity at the computational boundaries to generate a pulsating CSF flow [7].

Recently, significant advances in the visualization of the unsteady CSF flow in the ventricles inside the brain were made by the development of the Time-SLIP MRI (Time-Spatial Labeling Inversion Pulse Magnetic Resonance Imaging) medical imaging technology [8-10]. In the MRI Time-SLIP method, a non-selective inversion recovery pulse is applied to the entire field of view, followed by a selective inversion pulse that is applied to label the region to be examined, and images are acquired after a specified delay time. Time-SLIP MRI does not use bipolar gradients for quantification. It offers flexibilities to noninvasively select CSF flow region and visualize the flow at any angle, or location. A case that was studied by using the new Time-SLIP MRI technology involves imaging the ventricular CSF flows during a normal shaking of the head [9]. The Time-SLIP MRI images from the clinical study show that labeled CSF undergoes intensive mixing and the ventricular CSF flow in the brain can be readily altered by the head movement [9].

In the reported work, we have performed in silico CFD studies of the ventricular CSF flow excited by head nodding motions. Head nodding motion is an up-and-down movement of the head in the sagittal plane. Briefly, we used large-eddy simulations (LES) of the ventricular CSF flow in an anatomically accurate ventricle system that moves sinusoidally in the sagittal plane. Two head nodding motions were simulated. The first simulates heading nodding as in a common gesture to show agreement for about 0.1 G (or 10% of the Earth's gravity) acceleration at the cranial end of the aqueduct, or slow nodding. The second head motion simulated is related to hypnogogic jerks of the head when dozing off with 1 G acceleration, or fast nodding. To indicate fluid mixing, during the simulations, inertia-less particles of different colors were used to mark the CSF occupying the third ventricle, the aqueduct, and at the cranial end of the aqueduct prior to the commence of the simulation of the nodding. The computational model is physiologically accurate. The responses to the CSF flow to the head motion are reported and discussed.

#### NUMERICAL METHODOLOGIES

The anatomical structures of the ventricles are embryologically derived as the brain develops and the detailed anatomical features of the ventricles can vary from one subject to another. To digitally define anatomically accurate ventricular spatial regions in the heads of the subjects in this study, the T1-weighted MRI is used in the proposed studies. We obtain a subject T1-weighted MRI images of the brain and the neck. The MRI images are segmented and exported into CAD geometries [11]. We apply the ScanIP11 software to convert the MRI images to CAD files for the purpose of clearly defining the ventricular space where CSF flows.

The computational domain of the ventricular CSF flow conforms to the walls of the ventricular system obtained as described above. The anatomies of the four ventricles are complex and subject specific. A computational tool with efficient capabilities in mesh generation is required. The computational tool that is used in the proposed work is the STAR-CCM+ software [12]. The lateral apertures that link the fourth ventricle to the cerebellopontine cistern are the free flow boundaries. The inflow/outflow boundaries are set at the apertures with a pulsatile flow at the median aperture, which varies sinusoidally in time at 1 Hz. The volume flow rate is based on clinically measured values. The ventricular CSF flow is solved in a time-accurate manner.

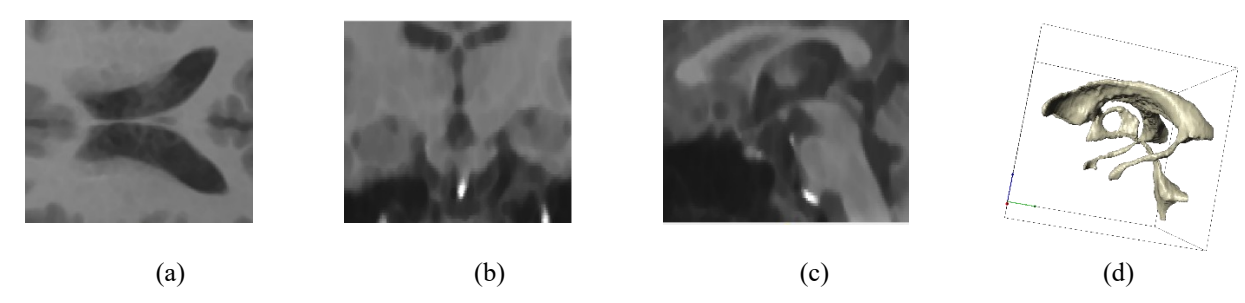
Since turbulent flow could present in the third ventricle, to fully revolve the flow fluctuations excited by the accelerative loading applied to the ventricles, LES computational simulations are performed. The Navier-Stokes equations solver is used for the LES simulations in this study. Cell-centered finite volume formulations are used on arbitrary cells. The second-order backward differencing is used for the discretization in time. The segregated Rhie-Chow SIMPLE based solver is applied in the proposed work. Second- and third-order schemes (central and upwind)

1ST INTERNATIONAL CONFERENCE FOR PURE SCIENCE (ICPS-2021), 26-27/MAY/2021, Diyala, IRAQ. To appear in AIP conference AIP conference publishing ISSN-0094-243x (2021)

for the convective fluxes are used in the current LES simulations. For the subgrid scale models, the wall-adapting local-eddy (WALE) eddy viscosity model is used.

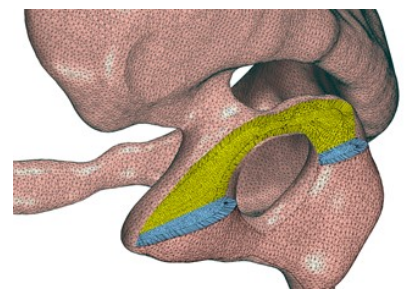
#### **RESULTS AND DISCUSSIONS**

Figure 1 (a), (b), and (c) show the representative slices of the MRI images of the ventricle. The resulting segmented CAD image of the ventricles is shown in Fig. 1 (d).



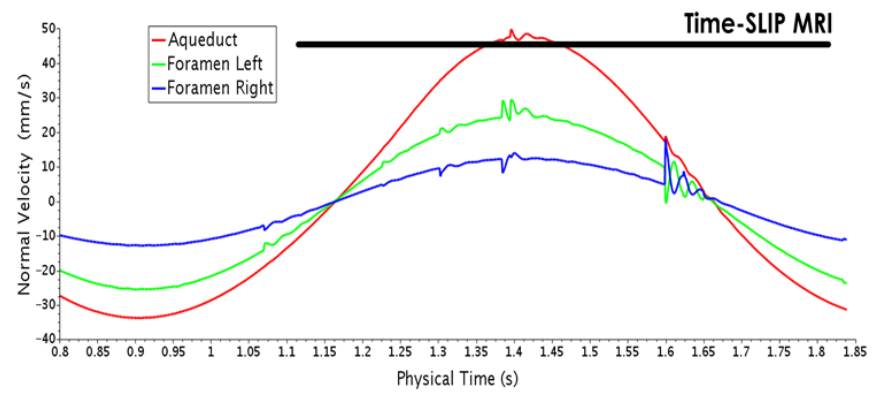
**FIGURE 1.** Segmentation of MRI images for the ventricles. (a) Transverse view, 9 (b) coronal view, 9 (c) sagittal view, 9 (d) reconstructed cad geometry of the ventricles.

Figure 2 shows unstructured meshes built by using the polyhedral volume cell and prism element layer near wall in the software with refinement near local features. The meshes are shown by removing the left lateral ventricle when generating the graphic so that the volume mesh in the third ventricle can be shown clearly. The meshes shown in Fig. 2 have been coarsened from that used in the actual computational simulations, so that individual mesh cell can be visible.



**FIGURE 2.** Computational mesh for the ventricular csf region showing the polyhedral volume mesh and the prism element layer mesh near wall on the two orthogonal planes that cut cross the third ventricle. Surface meshes on the walls of the right lateral ventricle and the third ventricle are shown. Meshes coarsened and the left lateral ventricle removed for demonstration purposes only.

Figure 3 shows the calculated variations of the maximum velocity through the left and the right Foremen and the throat of the aqueduct in a simulation with the head at rest. The corresponding speed measured at the aqueduct by using the Time-SLIP MRI is indicated by the coarse black line. The CFD calculated maximum CSF flow velocities in the cranial and the caudal directions are 51 mm/s and 35 mm/s, respectively. The measurement, which is the average of the cranial and the caudal flows, is 46 mm/s, which compares well with the averaged maximum velocity from CFD, which is 43 mm/s.



**FIGURE 3.** Ventricular CSF flow with head at rest.7 CFD calculated CSF flow velocities at the throat of the aqueduct in red, the left Foramen in green and the right Foramen in blue. Time-SLIP MRI measurement of 46 mm/s at the throat of the aqueduct is indicated in coarse black line. CFD velocities are the components normal to the planes defined by the local anatomic landmarks at these locations.

Inertia-less particles of different colors were used to mark the CSF occupying the third ventricle, the aqueduct, and at the cranial end of the aqueduct prior to the commence of the simulation of the nodding, as seen in Fig. 4 (a). After the simulations begin, snapshots of the particles locations at the same instant of time are taken and provided for stationary head in Fig. 4 (b), slow nodding in Fig. 4 (c), and fast nodding (hypnogogic jerk) in Fig. 4 (d). The particles distributions with the head in motions are more dispersed, showing that the head motions promote CSF mixing, as that observed in the Time-SLIP MRI scans. Further, the fast-nodding head motion is found to cause the mixing of CSF to be more uniform in the ventricular system and to transport the labeled CSF further into the lateral ventricle than the slow nodding and the no nodding do. The mixing of CSF and the transport in the ventricular CSF flows also occur at a faster time scale with the head in motion than at rest.

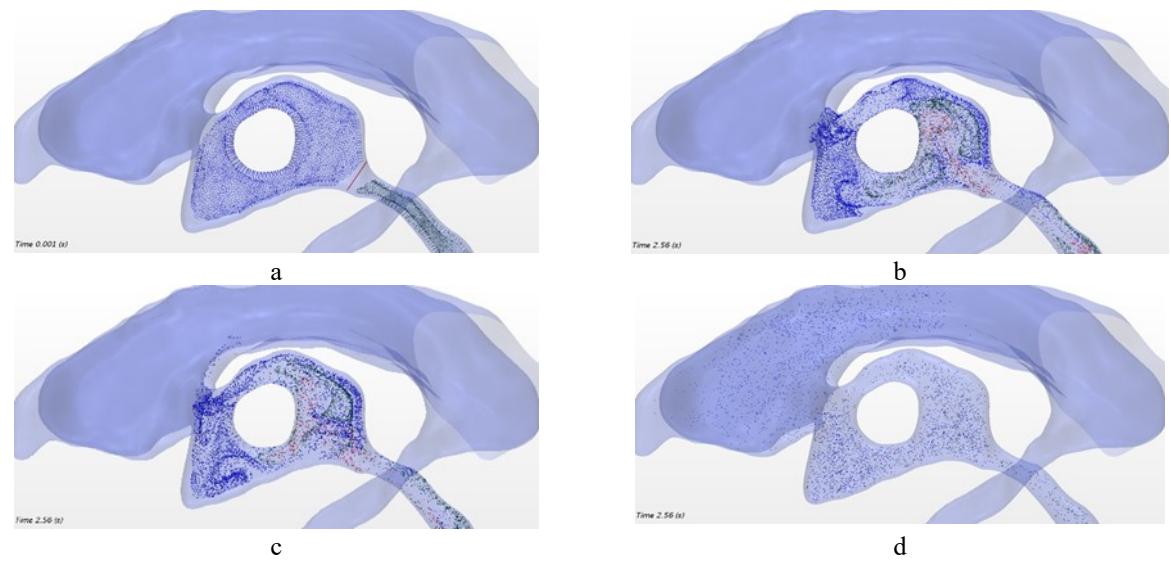
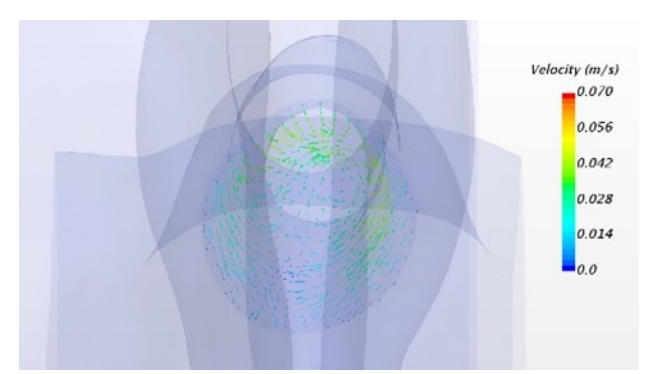


FIGURE 4. Preliminary CFD results: impacts of head motion on the ventricular CSF flow. Snapshots of color-coded inertialless particles marking CSF. Initially, CSF in the third ventricle is marked in blue, at the cranial end of the aqueduct in red, and in the aqueduct in green, as shown in (a). Enhanced mixing of the CSF due to the head motion are seen in (c) for slow nodding and (d) for fast nodding in comparison with that in head at rest (b). CSF flow in fast nodding has dispersed CSF to the lateral ventricles. The temporal horn of the left lateral ventricle is removed for viewing purposes only.

In Fig. 5, the CSF flow velocity vectors on an axial plane near the cranial end of the aqueduct are shown for the head jerk motion, or fast nodding. For a head at rest, the local flow is predominately axial, or along the aqueduct. The velocity vector plot shows that there are strong secondary flows induced by the nodding.

1ST INTERNATIONAL CONFERENCE FOR PURE SCIENCE (ICPS-2021), 26-27/MAY/2021, Diyala, IRAQ. To appear in AIP conference AIP conference publishing ISSN-0094-243x (2021)



**FIGURE 5.** Velocity vectors on a plane near the cranial end of the aqueduct. The vectors are colored by the magnitude of the velocity.

## **CONCLUSION**

Simulations for the head at rest and in nodding motions are performed. For the head at rest, where clinical data are available, the simulated CSF flow speeds in the aqueduct agree with Time-SLIP MRI results. The results of the simulation study presented show that the head nodding motions could modify the ventricular flow of CSF from that in brain at rest. In cases where the head motion is more rigorous, the head motion becomes a dominant driver of the CSF flow. The impacts of the head motions observed in the results include enhanced turbulent mixing of the CSF and the secondary flow induced in the narrow aqueduct. The findings could be significant in that the movement of the CSF flow deep inside the brain is influenced by head motion, which could have implication for the transport of nutrients as well as metabolic wastes in the brain.

#### **ACKNOWLEDGEMENT**

The authors are pleased to acknowledge that the work reported in this paper was performed with partial support of the US National Science Foundation Award 1723550.

#### REFERENCES

- 1. O. Faust, Documenting and predicting topic changes in Computers in Biology and Medicine: A bibliometric keyword analysis from 1990 to 2017, Informatics in Medicine Unlocked, Vol. 11, pp. 15-27, 2018.
- 2. T. Heldt and R. Mukkamala, Open Pacing Electrophysiol Ther Journal, Vol.3, pp. 45–54, 2010.
- 3. Y. Zhang, W. W. Liou and V. Gupta, Effects of excessive water intake on body-fluid homeostasis and the cardiovascular system A computer simulation, in *Emerging Trends in Computational Biology*, Bioinformatics, and Systems Biology Algorithm and Software Tools, 2016.
- 4. S. Ganpule, N. P. Daphalapurkar, K. T. Ramesh, A. K. Knutsen, D. L. Pham, P. V. Bayly and J. L. Prince, A three-dimensional computational human head model that captures live human brain dynamics. Journal of neurotrauma, Vol. 34, No. 13, pp. 2154-2166, 2017.
- B. Sweetman, M. Xenos, L. Zitella, et al., Computers in Biology and Medicine, Vol. 41, No. 2, pp. 67-75, 2011.
- 6. S. Cheng, M. Stoodley, J. Wong, Journal of Biomechanics, Vol. 45, No. 7, pp. 1186-1191, 2012.
- 7. W. W. Liou, Y. Yang and S. Yamada, 6th International Conference on Computational and Mathematical Biomedical Engineering, Tohoku University, Japan, pp. 10-12 June 2019.
- 8. S. Yamada, M. Miyazaki, H. Kanazawa, et al., Radiology, 249 (2), 644-652 (2008).
- 9. S. Yamada. Croatian Medical Journal, 55(4), 337-346 (2014).
- 10. S. Yamada and E. Kelly, "Cerebrospinal fluid dynamics and the pathophysiology of hydrocephalus: new concepts," in *Seminars in Ultrasound, CT and MRI* (WB Saunders, 2016) **37**, 2, pp. 84-91.
- 11. Retrieved from https://www.synopsys.com/simpleware.html.
- 12. Retrieved from https://www.plm.automation.siemens.com/global/en/products/simcenter/STAR-CCM.html.